Improved white matter tract segmentation reproducibility using global diffusion tensor neighborhood tractography

Paul Armitage[1], Susana Muñoz Maniega[2], James Bridson[2], Michael Poon[2], and Mark Bastin[2]
[1]*University of Sheffield, Sheffield, South Yorkshire, United Kingdom,* [2]*University of Edinburgh, Edinburgh, United Kingdom*

Introduction: Despite the widespread use of diffusion imaging, consistent and reliable extraction of white matter pathways in the human brain is still a challenging proposition. The neighborhood tractography (NT) approach [1,2] offers the potential to improve the reliability of tract extraction, overcoming some of the limitations of manually seeded or guided approaches, by providing fully automated tract segmentation. In this study, a previously described approach, using NT in conjunction with a global tractography algorithm [3], was evaluated in terms of the reproducibility of extracted tract volume, mean diffusivity <D> and fractional anisotropy FA. In addition, the success of the tract extraction was evaluated qualitatively using a visual tract quality score (TQS).

Methods: NT was implemented using a modified version of fast marching tractography (FMT) [4], extended to better account for multiple fiber partial volume effects by using the full information contained in the diffusion tensor [3]. Seed voxels were defined in standard brain space for several white matter fibers and transposed into the native space of each individual subject using the transformation matrix obtained from affine registration of the subject's T_2-weighted EPI image to the ICBM-152 template. A 3D neighborhood ($7 \times 7 \times 7$) was defined around the native space seed voxel, and the FMT algorithm run to obtain connectivity maps for each neighborhood voxel, which were compared to a reference connectivity map [5] for the pathway of interest by using normalized cross-correlation. Maps originating from each neighborhood voxel were then ranked by similarity to the reference with the most similar map being chosen as that representative of the pathway(s) of interest. A tract segmentation was then obtained by thresholding the resulting optimum connectivity map at an empirically chosen value of 0.7. To evaluate the intra- and inter-subject reproducibility of the resulting tract volume, <D> and FA, diffusion tensor imaging data was acquired on three separate occasions (not more than a month apart) from seven healthy volunteers (mean age: 32 ± 5 yrs) on a GE Signa HDXT 1.5T clinical scanner using 64 non-collinear gradient directions (TR / TE = 16500 / 95.5 ms, 128 × 128 matrix, 256 × 256 mm FOV, 2mm slice thickness). The NT algorithm described above was applied to each subject by seeding in the genu and splenium of the corpus callosum, the left cingulum bundle and the left corticospinal tract. For each segmented white matter tract, the resulting volume, <D> and FA were compared to those obtained directly by seeding from the native space seed voxels obtained by registration alone. The individual extracted pathways were also classified visually with a TQS on a scale ranging from 1-7, using the criteria defined in Fig. 1.

Results: Table 1 summarizes the percentage coefficients of variation in tract volume and tract averaged <D> and FA obtained by performing tractography with seed points placed using direct affine registration and by optimization using NT. Data is shown for intra-subject reproducibility obtained from the three repeat scans in each of the seven individuals and for inter-subject reproducibility across all seven individuals. The mean TQS, averaged over all subjects and fibers, was 2.94 for direct affine registration with 49% having a TQS ≤ 2, while mean TQS was 1.76 with 83% having TQS ≤ 2 using NT. Figure 2 illustrates the average connectivity maps obtained from all 7 subjects for each fiber along with their respective template reference maps.

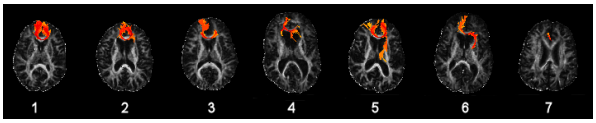

Figure 1. Example images corresponding to different.TQS shown for transverse projections of the corpus callosum genu where; 1 indicates a good representation; 2 good + minor branches; 3 partial tract; 4 partial tract + minor branches; 5 good + major branches; 6 partial + major branches; 7 poor representation.

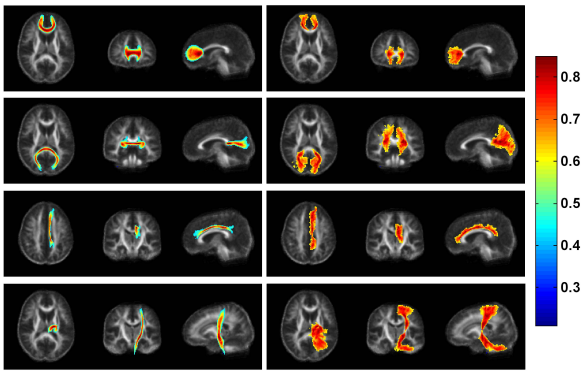

Figure 2. Template reference maps (left) and average optimum connectivity maps generated using NT (right) for each of the four fibres; corpus callosum genu (top row); corpus callosum splenium (2nd row); cingulum (3rd row); and corticospinal tract (bottom row).

		Direct Registration			Global NT		
		Vol	<D>	FA	Vol	<D>	FA
Intra-subject	Genu	28.5	7.8	8.0	18.9	2.5	4.8
	Splenium	44.4	4.0	7.8	19.2	3.2	7.5
	Cingulum	59.3	4.1	10.1	35.6	3.2	8.7
	Corticospinal	29.2	3.3	6.2	24.8	2.8	5.0
Inter-subject	Genu	44.0	2.4	6.9	16.1	3.4	10.0
	Splenium	58.7	7.9	8.2	33.4	2.4	6.1
	Cingulum	45.9	2.1	13.7	38.9	3.2	6.4
	Corticospinal	23.3	3.8	8.5	17.7	4.3	7.9

Table 1. Intra- and inter-subject percentage coefficients of variation in tract volume (Vol) and tract-averaged <D> and FA from seed voxels defined by direct affine registration and global NT.

Discussion: The NT approach to automated tract segmentation significantly reduces the variability in measurements of tract volume, <D> and FA when compared to performing tractography from seed voxels defined by direct registration from a template. Using this approach, 83% of fibers were considered to provide acceptable representations of the fasciculi of interest, compared to only 49% for directly registered seed voxels. The resulting percentage coefficients of variation in the measured parameters compare favorably to those obtained in previous studies, including those that use manual methods [6,7,8]. Possible future improvements to the method include implementing a more sophisticated segmentation of the connectivity map than fixed thresholding, and developing multi-voxel seeding strategies to overcome the tendency for the fiber width to narrow to a single voxel when in close proximity to the seed voxel. This narrowing could result in an underestimation of tract volume and cause the fiber to 'disappear' in thresholded average connectivity maps such as those shown in Fig. 2, as the spatial averaging exaggerates the effect.

References: [1] Clayden JD, et al. *Neuroimage* 2006;33:482-92. [2] Clayden JD, et al. *IEEE Trans Med Imaging* 2007;26:1555-61. [3] Armitage et al., *Proc ISMRM* 2009. [4] Parker GJ, et al. *IEEE Trans Med Imaging* 2002;21:505-512. [5] Mori S, et al. Elsevier. [6] Cicarelli et al., *Neuroimage* 2003;18:348-359. [7] Clayden JD et al., *Neuroimage* 2009;45:377-385. [8] Heiervang E et al., *Neuroimage* 2006;33:867-877.

Acknowledgements: All imaging was performed at the Brain Research Imaging Centre, University of Edinburgh.